Int. J. Electrochem. Sci., 9 **(2014)** 4086 - 4103

International Journal of
ELECTROCHEMICAL
SCIENCE
www.electrochemsci.org

Synergistic Effect of Halides on the Corrosion Inhibition of Mild Steel in H_2SO_4 by a Triazole Derivative: Kinetics and Thermodynamic Studies.

O. A. Hazazi[1], *A. Fawzy*[1,2], *M. Awad*[1,3,*]

[1] Chemistry Department, Faculty of Applied Sciences, Umm Al-Qura University, Makkah Al-Mukarramah, 13401, Saudi Arabia Kingdom.
[2] Chemistry Department, Faculty of Science, Assiut University, Assiut, 71516 Egypt.
[3] Chemistry Department, Faculty of Science, Cairo University, Gizah, Egypt.
[*]E-mail: mawad70@yahoo.com.

Received: 13 February 2014 / *Accepted:* 10 April 2014 / *Published:* 19 May 2014

The synergistic effect between 4-amino-5-methyl-4*H*-1,2,4-triazole-3-thiol (AMTT) and halides on the corrosion of mild steel in 0.5 M H_2SO_4 solution at 20 ^oC is investigated by potentiodynamic polarization and electrochemical impedance spectroscopy (EIS). Experimental results revealed the significant synergistic action of halides on the protective effect of AMTT. Both protection efficiency (%*P*) and degree of surface coverage (θ) increase with increasing AMTT concentration, and the effect of halides on the protection efficiency follow the trend: $Cl^- < Br^- < I^-$ indicating that the radii and electronegativity of the halide play a prominent role in the adsorption process. In contrary the synergism followed the reverse order due to the effective inhibition efficiency of iodide. The adsorption of the AMTT accords with the Temkin adsorption isotherm. Some thermodynamic and kinetic parameters have been calculated and discussed.

Keywords: Corrosion inhibitor; Temkin isotherm; Mild steel; Halide ions; Adsorption

1. INTRODUCTION

Acid solutions are generally used for the removal of undesirable scale and rust in the metal working, cleaning of boilers and heat exchangers. However, in such harsh media metals severely corrode. To avoid the dissolutions of metals, organic inhibitors should be added to protect those metals from dissolution. Corrosion inhibitors effectively eliminate the undesirable destructive effects of aggressive media and prevent iron dissolution. A perusal of the literature on acid corrosion inhibitors reveals that most of the well-known corrosion inhibitors contains nitrogen, sulfur, and oxygen atoms with nitrogen containing organic compounds as an efficient inhibitors in HCl solution and those with

sulfur containing compounds as efficient inhibitors in H_2SO_4 solution [1-10]. Compounds containing both nitrogen and sulphur can provide excellent corrosion protection efficiency compared with compounds containing either nitrogen or sulphur [1,2,11].

On the other hand, triazoles (heterocyclic compounds containing N and S) have been reported as an effective corrosion inhibitors [7-9,12-14]. In addition, it has been reported that many N- and S-containing triazole derivatives are environmentally friendly corrosion inhibitors [12,13]. The inhibition efficiency could be increased by what is the so-called synergism; adding a low cost species to the organic inhibitor for the sake of enhancing the adsorption of the organic inhibitor via the formation of a bridge; a previously adsorbed anions enhances the adsorption of positively charged inhibitors increasing the inhibition efficiency. Synergistic inhibition is an effective means to improve the inhibitive effect of an inhibitor via enhancing its adsorption through ion-pair interactions, to decrease the amount of usage, to diversify the application of an inhibitor [15-20]. In this work the inhibition efficiency of 4-amino-5-methyl-4*H*-1,2,4-triazole-3-thiol (AMTT) on the corrosion of mild steel in 0.5 M H_2SO_4 is studied. Control of corrosion extend the life of the equipment, and suppress the dissolution of environmentally toxic metals from components. Also the synergistic action of halides on the corrosion inhibition of steel by AMTT is studied.

2. EXPERIMENTAL

2.1. Mild steel sample

Tests were performed on mild steel of the following composition (wt. %): 0.07% C, 0.29% Mn, 0.07% Si, 0.012% S, 0.021 % P and the remainder iron. Samples of 0.5 cm^2 were used.

2.2. Inhibitor

AMTT inhibitor of structure shown below was synthesized as reported elsewhere [21]. Sodium halides were obtained from Aldrich and used as received.

2.3. Solutions

The solution of 0.5 M H_2SO_4 was prepared by dilution of AR grade 98% H_2SO_4. Stock solutions of AMTT and sodium halides were prepared in 0.5 M H_2SO_4 and the desired concentrations were obtained by appropriate dilution.

2.4. Electrochemical measurements

Electrochemical experiments were carried out in a conventional three-electrode cell with a platinum counter electrode (CE) and a $Hg/Hg_2SO_4/SO_4^{2-}$ coupled to a fine Luggin capillary as the

reference electrode (RE). Potential values are represented with respect to the saturated calomel electrode. In order to minimize the ohmic contribution, the Luggin capillary was kept close enough to the working electrode (WE) which was fitted into a glass tube of proper internal diameter by using epoxy resins. The WE surface area of 0.5 cm^2 was abraded with emery paper down to grade 2000 on test face, rinsed with distilled water, degreased with acetone, and dried with a cold air stream. Before measurements the electrode was immersed in the test solution at open circuit potential (E_{OCP}) for 15 min at 20 ^oC or until the steady state is obtained. All electrochemical measurements were carried out using PGSTAT potentiostat/galvanostat. Potentiodynamic polarization curves were scanned in the potential range of E_{OCP} ± 250 mV at a scan rate of 2 mV/s. Current densities were calculated on the basis of the apparent geometrical surface area of the electrode. The measurements were repeated at least three times to test the reproducibility of the results.

3. RESULTS AND DISCUSSION

3.1. Open circuit potential (E_{OCP})

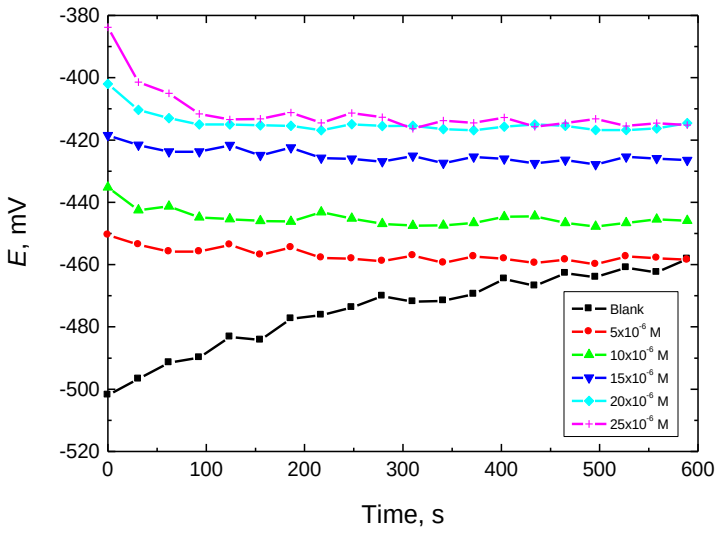

Figure 1. Open circuit potential, E_{OCP} vs. time relations for mild steel immersed in 0.5 M H_2SO_4 in the absence and presence of AMTT inhibitor at 20 ^oC.

Figure 1 shows the change of E_{OCP} with time obtained at mild steel in 0.5 M H_2SO_4 both in the absence and presence of various concentrations of AMTT ion at 20 ^oC. Inspection of this figure reveals several interesting points;

1. As can be seen E_{OCP} in the blank solution started at -503 mV then shifted anodically and the steady state is obtained after *ca*. 10 min. This indicates the initial dissolution process of the air formed oxide film and the attack on the bare metal.

2. In the presence of AMTT, the E_{OCP} started at relatively positive potential compared with that in the absence of the inhibitor and then shifted cathodically. The steady state is attained rapidly, compared with the blank. With increasing the concentration of the inhibitor the shift in the open circuit potential increases in the active direction pointing to that the inhibitor might act mainly as an anodic inhibitor. According to Riggs [22], the classification of a compound as an anodic or cathodic type inhibitor is based on the E_{OCP} displacement; if the shift in E_{OCP} is at least ±85 mV compared to the one measured in the blank solution it can be classified as an anodic or cathodic inhibitor. However, from Fig. 1 the shift in E_{OCP} on adding AMTT is about 55 mV revealing that the present inhibitor act as a mixed type inhibitor.

The initial positive shift could be attributed to the adsorption of the inhibitor and the partial attraction of electrons by nitrogen and/or sulfur atom with high electronegativity in the inhibitor decreasing the electron density on the iron.

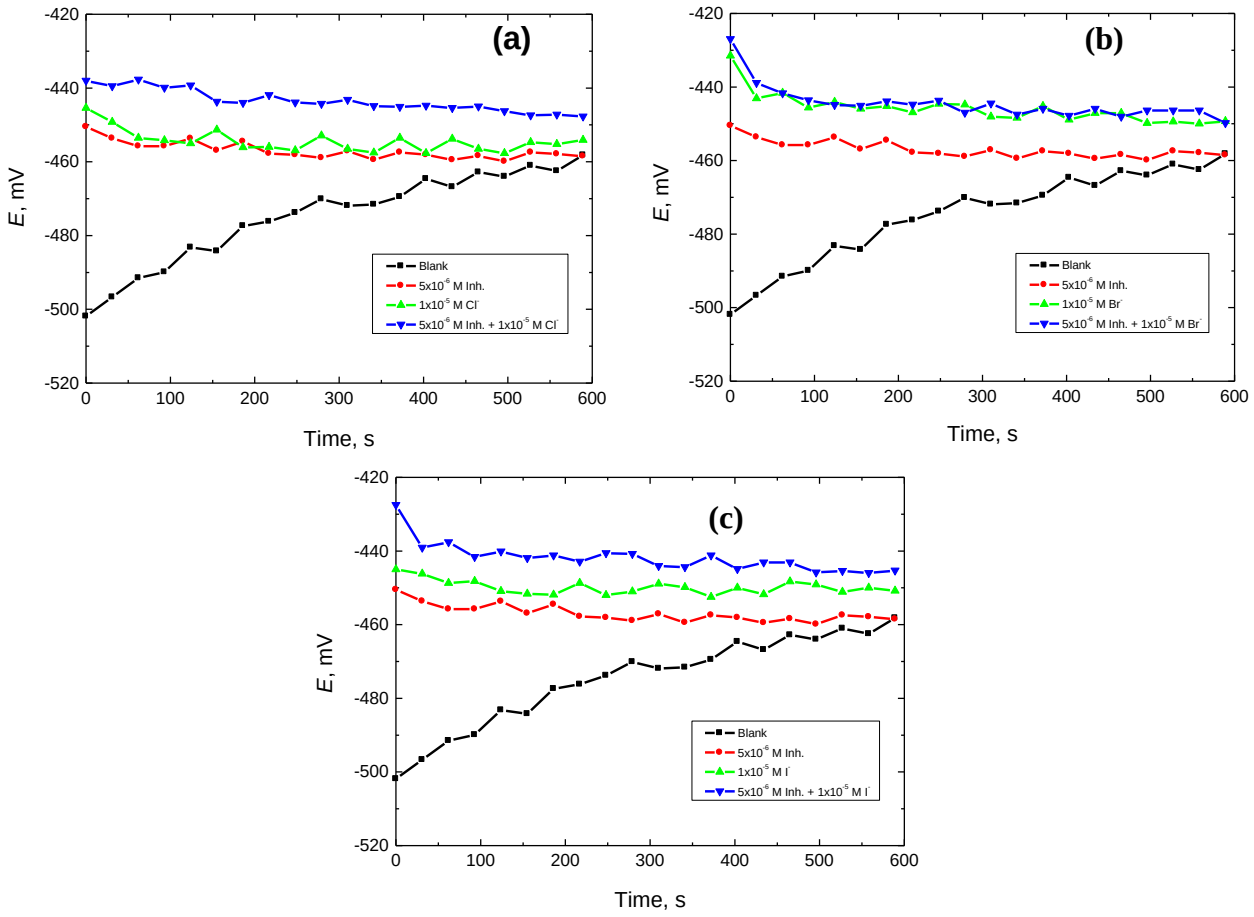

Figure 2(a-c). Open circuit potential, E_{OCP} vs. time relations, for mild steel in 0.5 M H_2SO_4 in the absence and presence of AMTT inhibitor and $1x10^{-5}$ M halide; (a) for NaCl, (b) for NaBr and (c) for NaI.

The variation of E_{OCP} of mild steel in the absence and presence of the inhibitor and/or halides was followed as a function of time as shown in Fig. 2(a-c). The E_{OCP} vs. time curve for the blank shift to the less negative direction and takes around 10 min to attain the steady state as mentioned above.

When the inhibitor and/or halide ions are/is added, the E_{OCP} starts at relatively positive potential compared with that in the absence of both species and the steady state takes shorter time to be attained. The E_{OCP} in the presence of any of the two species or in the presence of both is relatively positive compared with the blank. However the shift is not that much to classify the inhibitor as an anodic or cathodic one according to Riggs [22].

3.2. Polarization Measurements

Figure 3 shows the potentiodynamic polarization curves for mild steel in 0.5 M H_2SO_4 in the absence and presence of various concentrations of AMTT at 20 ^oC. Polarization parameters including corrosion potential, E_{corr} , corrosion current density, I_{corr} , Tafel slopes, β_c and β_a and the percentage protection efficiency (%P) derived from this Figure are given in Table 1. The effect of AMTT inhibitor on the anodic branch is significant; the anodic branch bodily shifted to lower currents while the effect on the cathodic branch is comparatively lower. Also the corrosion potential shifts to anodic direction and the shift increases with increasing the concentration consistently with the results in Fig.1. The effect of inhibitor concentration on the Tafel slopes is not significant indicating that the inhibitor exerts its action via simple blocking, and that the adsorption of the inhibitor does not change the mechanism [23].

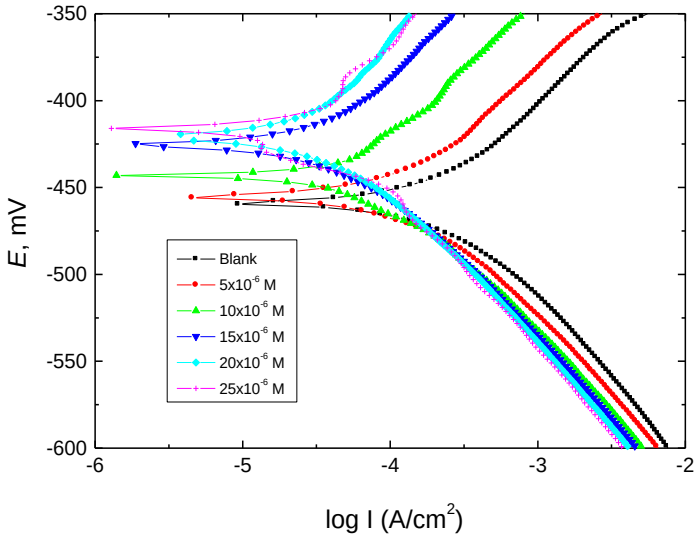

Figure 3. Potentiodynamic polarization curves for mild steel in 0.5 M H_2SO_4 in the absence and presence of AMTT inhibitor at 20 ^oC.

The percentage protection efficiency, %P listed in Table 1 is calculated by the following equation

$$\%P = \left[1 - \frac{i_{corr1}}{i_{corr2}}\right] 100 \qquad (1)$$

where i_{corr1} and i_{corr2} are corrosion current densities in the presence and absence of inhibitor, respectively. Figure 4 shows the dependence of the protection efficiency on the inhibitor concentration. The plot is of sigmoid shape; i.e. %*P* increases with the concentration until it reaches a plateau at protection efficiency *ca.* 94% indicating the significant protection of the present inhibitor under the present conditions.

Table 1. Polarization data for mild steel in 0.5 M H_2SO_4 with AMTT inhibitor at 25 ^oC.

10^6 [AMTT] M	E_{corr} (mV)	β_c (mV/dec)	B_a (mV/dec)	I_{corr} ($\mu A/cm^2$)	θ	% *P*
0	-461	102	83	201	--	--
5	-456	96	81	132	0.34	34
10	-443	97	74	55	0.62	62
15	-425	96	76	32	0.81	81
20	-419	94	78	17	0.92	92
25	-415	93	79	12	0.94	94

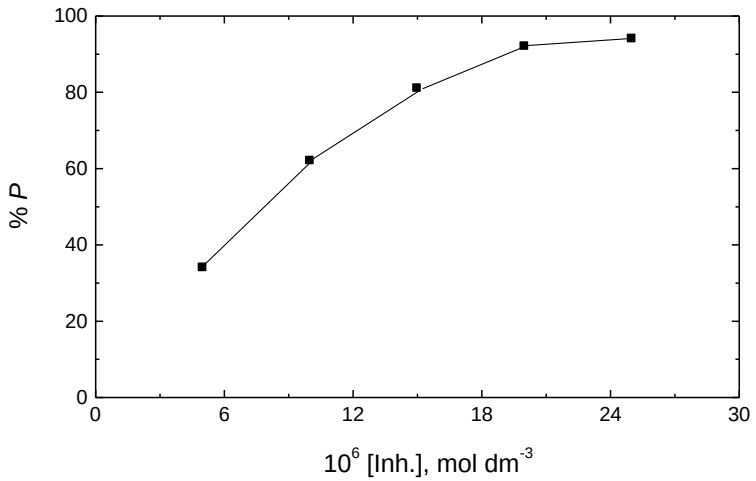

Figure 4. Dependence of the protection efficiency (%*P*) on AMTT inhibitor concentration for mild steel in 0.5 M H_2SO_4 at 20 ^oC.

Figure 5 shows the polarization curves for mild steel in 0.5 M H_2SO_4 in the absence and presence of $5x10^{-6}$ M AMTT and/or $1x10^{-5}$ M of halide ions. It is clear that the mild steel corrosion is slightly inhibited in the presence of either a small concentration of inhibitor or halide ions. The polarization parameters extracted from this figure are given in Table 2. In the presence of lower concentrations of individual species (inhibitor or halide ions), the effect on E_{corr} and I_{corr} is not significant. In the presence of halide ions only a slight decrease in the corrosion rate i.e., slight shifts in both anodic and cathodic currents are obtained. This could be ascribed to adsorption of halide over the corroded surface [24]. In other words, both cathodic and anodic reactions of mild steel are slowly retarded by halides. In the presences of iodide only, the inhibition is significant. Generally, the

adsorbability of anions is related to the degree of hydration. The less hydrated ion is preferentially adsorbed on the metal surface. The ease of adsorption (greater protection efficiency) shown in the case of the iodide ions may be due to its less degree of hydration. The protective effect of halide ions is found to be in the same order as that of adsorption ability [17]. In the coexistence of both species, however, the anodic branch is significantly shifted to lower currents. The considerable increase in the inhibition of corrosion in the coexistence of inhibitor and halide ions points to the co-operative adsorption of both species.

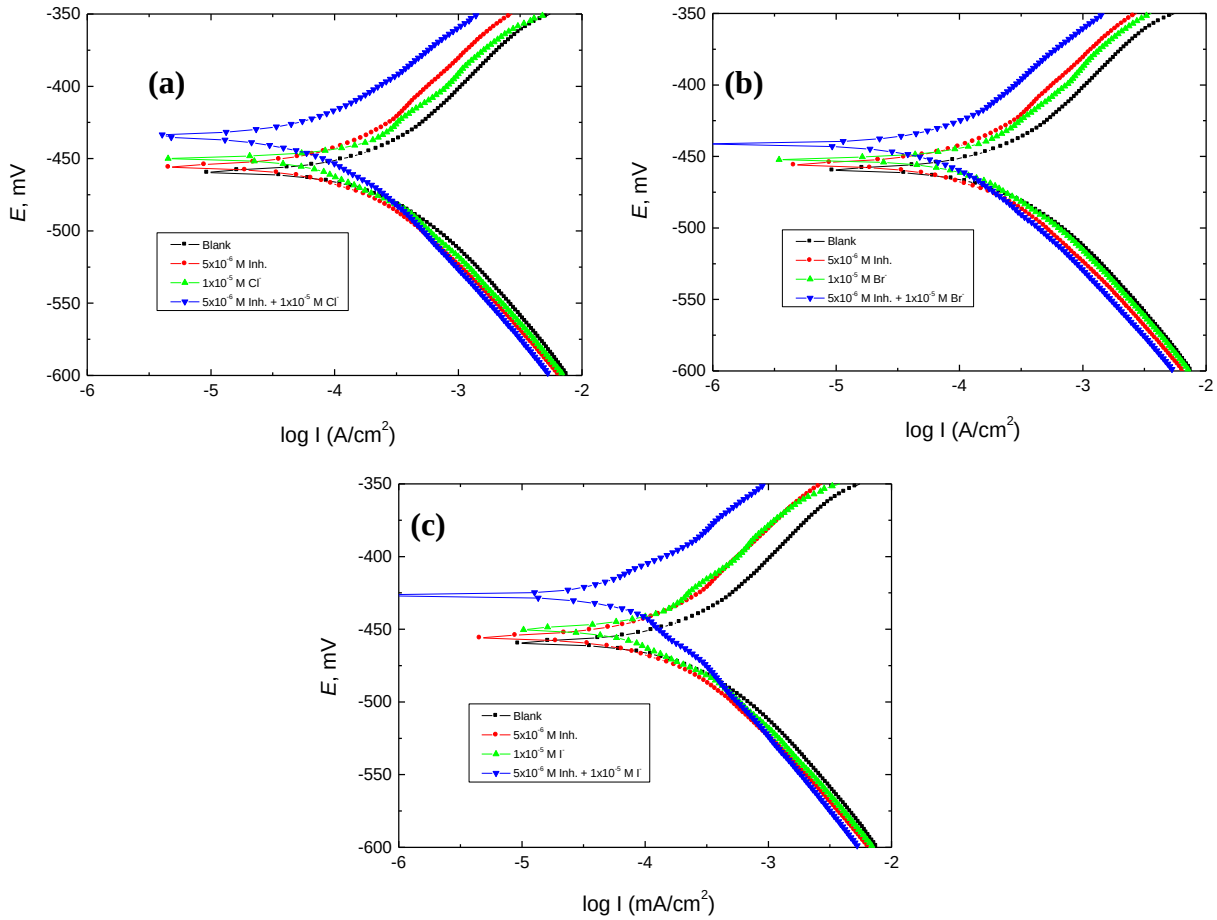

Figure 5(a-c). Potentiodynamic polarization curves for mild steel in 0.5 M H_2SO_4 in the absence and presence of AMTT inhibitor and $1x10^{-5}$ M halide; (a) for NaCl, (b) for NaBr and (c) for NaI.

Figure 6 illustrates the dependence of the protection efficiency on halide concentration coexisting with a constant concentration of the inhibitor. As can be clearly seen increasing the concentration of halide increases the inhibition efficiency even though the inhibitor concentration is constant. At the same concentration of halides the increase in the protection efficiency is as follows: I^- > Br^- > Cl^- consistently with the arrangement of the inhibition efficiency in the presence of halides; in the same order of the radius and degree of hydration of halides.

Table 2. Polarization data and synergism parameter for AMTT inhibitor and halides on mild steel in 0.5 M H_2SO_4 at 20 ^oC.

Medium	E_{corr} (mV)	β_c (mV/dec)	β_a (mV/dec)	I_{corr} ($\mu A/cm^2$)	% *P*	θ	S_θ
Blank	-461	102	83	201	--	--	
$5x10^{-6}$ M AMTT	-456	96	81	132	34	0.34	
$1x10^{-5}$ M Cl^-	-451	95	71	171	15	0.15	
$5x10^{-6}$ M AMTT + $1x10^{-5}$ M Cl^-	-447	93	73	52	74	0.74	2.16
$1x10^{-5}$ M Br^-	-455	91	79	143	29	0.29	
$5x10^{-6}$ M AMTT + $1x10^{-5}$ M Br^-	-448	93	74	46	77	0.77	2.01
$1x10^{-5}$ M I^-	-451	96	73	123	39	0.39	
$5x10^{-6}$ M AMTT + $1x10^{-5}$ M I^-	-445	93	69	42	79	0.79	1.92

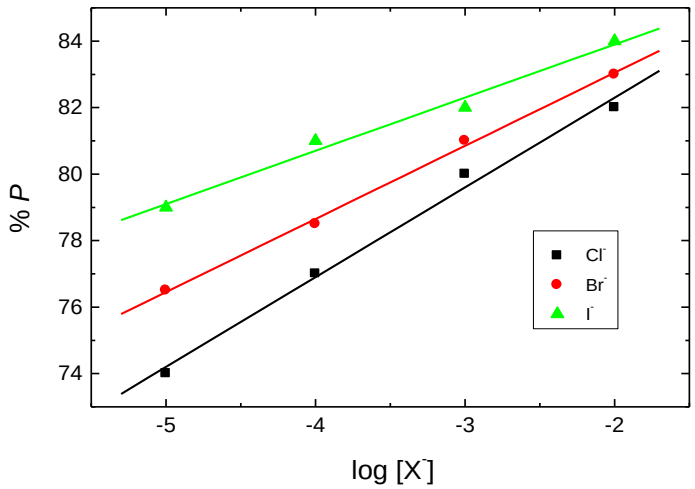

Figure 6. Effect of halide ion concentration on %*PI* for mild steel in 0.5 M H_2SO_4 containing $5x10^{-6}$ M AMTT inhibitor at 20 ^oC.

3.4. Synergism

There are several controlling factor for the inhibiting effect of organic inhibitors such as the molecular structure of the organic compounds, surface charge density and the potential of zero charge of the metal. The adsorption of a cationic inhibitor is expected to be enhanced by increasing the negative charge density on the metal surface. Thus the pre-adsorption of a halide could enhance the adsorption of the cationic inhibitor due to ion–pair interactions between the molecules and the halide ions, resulting in what is the so-called inhibition synergism. Halide ions interconnect the positively charged inhibitor and the positively charged electrode (under the present conditions). In other words the inhibitor molecules are protonated and thus the pre-adsorption of halides on the metal surface

enhances the inhibitor adsorption. This interaction can be quantized by a parameter called synergism parameter (S_θ) [25,26] which is defined as,

$$S_\theta = 1\text{-}\theta_{1+2} / 1\text{-}\theta'_{1+2} \quad (2)$$

where: $\theta_{1+2} = (\theta_1 + \theta_2) - (\theta_1\theta_2)$; θ_1 and θ_2 are the degrees of surface coverage in the presence of the halide ion and the AMTT, respectively, and θ'_{1+2} is the degree of surface coverage in the presence of both species. S_θ approaches unity when no interaction takes place between the inhibitor molecules and the halide ion. At $S_\theta > 1$, a synergistic effect is obtained as a result of a co-operative adsorption. In the case of $S_\theta < 1$, antagonistic behavior prevails due to a competitive adsorption [27]. Figure 7 shows the effects of halides ions concentration on S_θ estimated in the presence of 0.5 M H_2SO_4 solution containing $5x10^{-6}$ M AMTT and different concentration of halides. The S_θ values are found to be higher than unity, suggesting a real synergistic action of halide ion with the inhibitor. The above results reveal that AMTT can act as an effective inhibitor in the presence of halide ions even at low concentrations of AMTT inhibitor. The obtained S_θ is in the order: $Cl^- > Br^- > I^-$ while the protection efficiency is in the order: $Cl^- < Br^- < I^-$ in agreement with literature [28,29]. This could be explained on the basis that the inhibition efficiency in the presence of iodide is relatively high, compared with the bromide and chloride.

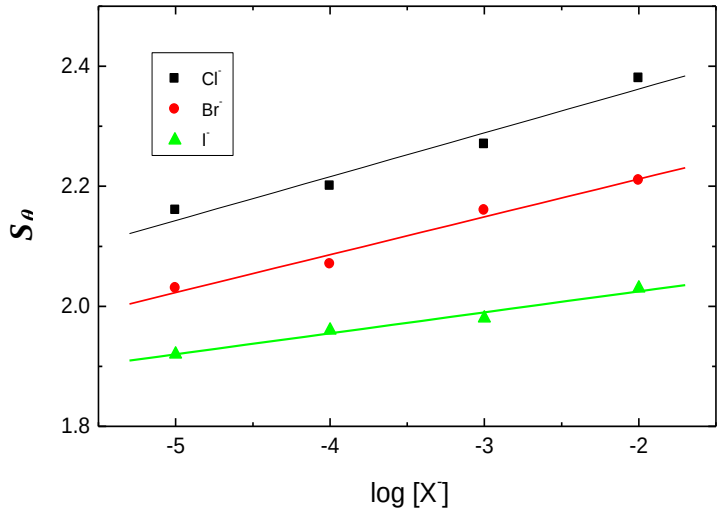

Figure 7. Effect of halide ion concentration on the synergism parameter (S_θ) obtained for mild steel in 0.5 M H_2SO_4 containing $5x10^{-6}$ M AMTT inhibitor at 20 ^oC.

3.4. Electrochemical impedance spectroscopy (EIS)

Figure 8 shows Nyquist plots of steel in 0.5 M H_2SO_4 both in the absence and presence of various concentrations of AMTT at 20 ^oC after 30 min of immersion. The charge transfer resistance (R_{ct}) values are calculated from the difference in impedance at lower and higher frequencies [30]. The inhibition efficiency obtained from the charge transfer resistance is calculated by the following equation

$$\% P = \left[\frac{(1/R_{ct})_0 - (1/R_{ct})}{(1/R_{ct})_0} \right] 100 \qquad (3)$$

where $(R_{ct})_0$ and (R_{ct}) are the values of charge transfer resistance in the absence and presence of the inhibitor, respectively. As can be seen depressed semicircles are obtained in the presence of various concentrations of AMTT and the radius of those circles are concentration sensitive, it increases significantly with increasing concentration of AMTT. The Nyquist plots at high frequencies are not perfect semicircles and this difference has been attributed to frequency dispersion as a result of roughness of the electrode surface [31]. This anomalous phenomenon can be attributed to the inhomogeneity of the electrode surface arising from surface roughness or interfacial phenomena [32]. Charge transfer resistance (R_{ct}) and inhibition efficiency (%*P*) values are given in Table 3. Interestingly, a high consistency between the results obtained by impedance measurements and polarization curves are shown (compare last columns in Tables 1 and 3).

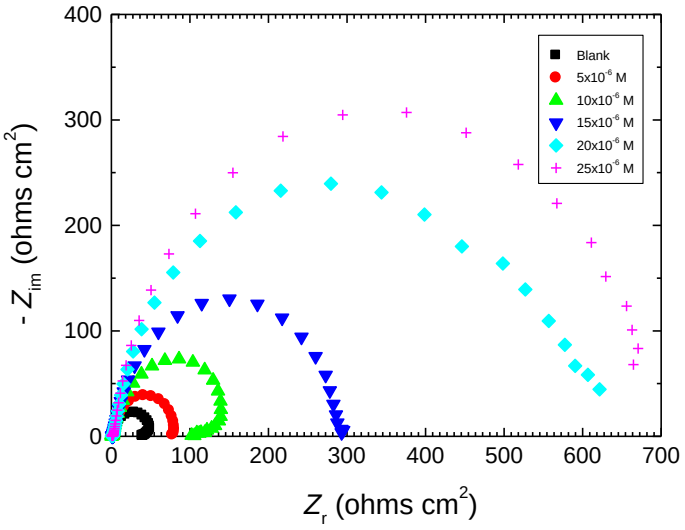

Figure 8. Nyquist plots for mild steel in 0.5 M H_2SO_4 in the absence and presence of AMTT inhibitor at 20 ^oC.

Table 3. Polarization resistance and protection efficiency for corrosion of mild steel in 0.5 M H_2SO_4 containing AMTT inhibitor at 20 ^oC.

10^6 [AMTT], M	R_{ct} (ohms cm^2)	% *P*
0	52	--
5	80	35
10	138	62
15	297	82
20	634	92
25	661	93

Figure 9 shows impedance plots for mild steel in 0.5 M H_2SO_4 in the absence and presence of $5x10^{-6}$ M AMTT and/or $1x10^{-5}$ M of halide ions. The charge transfer resistance obtained in the presence of either a small concentration of inhibitor or halides are slightly longer than that of the blank. The presence of inhibitor with halide tremendously increases the radius of the semicircle in the Nyquist plots. For instance, R_{ct} equals to 52 ohms cm^2 for the blank solution and 61, 79 and 191 ohms cm^2 in the presence of AMTT, Cl^- and AMTT + Cl^-, respectively. The charge transfer resistance in the co-existence of the two species is more than double compared with that obtained in the individual presence of AMTT or halide ions. Again this confirms the high protection efficiency of AMTT, especially in the presence of halides which enhance the adsorption of AMTT via the formation of a bridge in which halide ions are initially adsorbed on the electrode surface followed by the adsorption of the inhibitor.

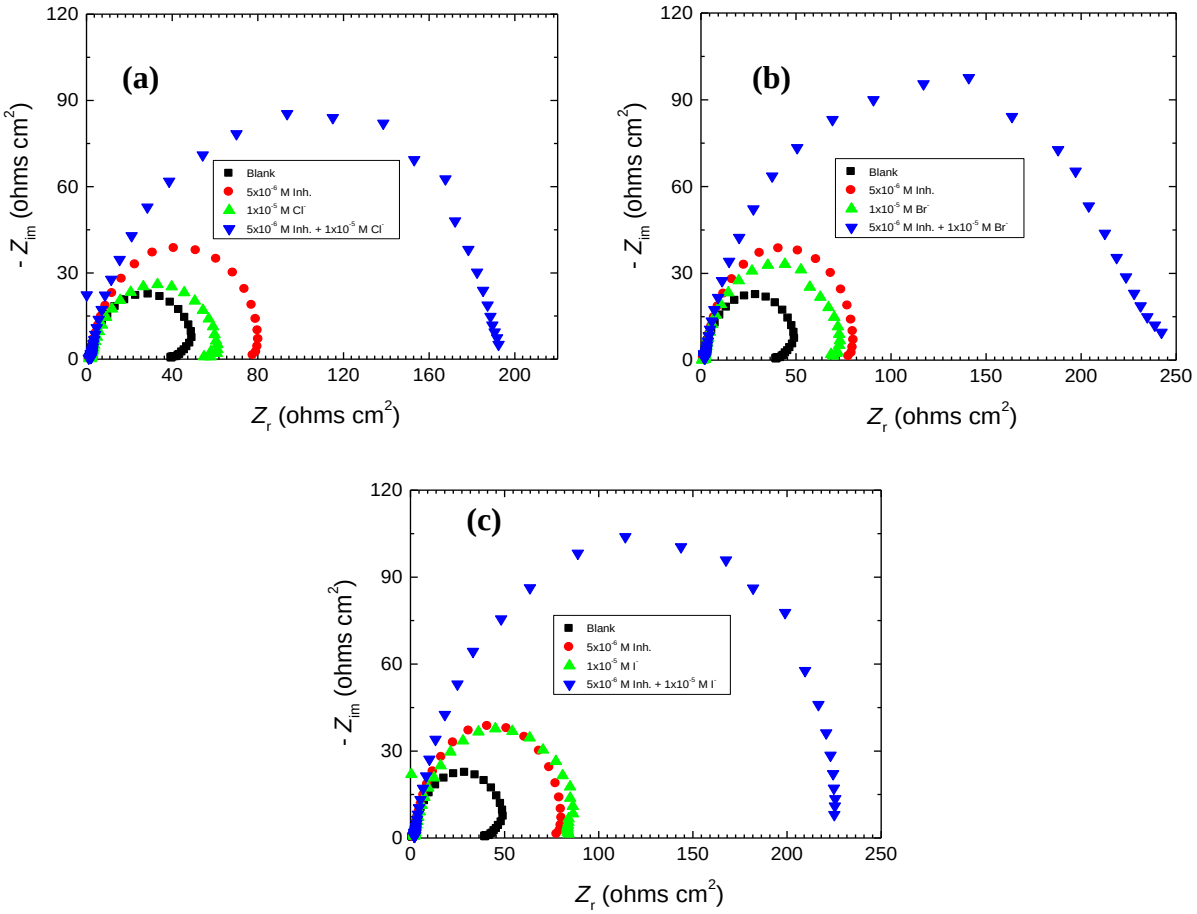

Figure 9(a-c). Nyquist plots for mild steel in 0.5 M H_2SO_4 in the absence and presence of AMTT inhibitor and $1x10^{-5}$ M halide; panel (a) for NaCl, panel (b) for NaBr and panel (c) for NaI.

Figure 10 shows Nyquist plots for steel in 0.5 M H_2SO_4 containing constant concentration of AMTT and different concentrations of halides. The semi-circle radius in the presence of $5x10^{-6}$ M AMTT is so small. On adding halides the radius increases reflecting the increase in the inhibition efficiency as shown in Table 4. For instance the protection efficiency in the presence of AMTT only

equals 35% and in the presence of the same concentration of AMTT after adding $1x10^{-2}$ M Cl^- equals to 80% confirming the synergism in consistent with polarization results shown above.

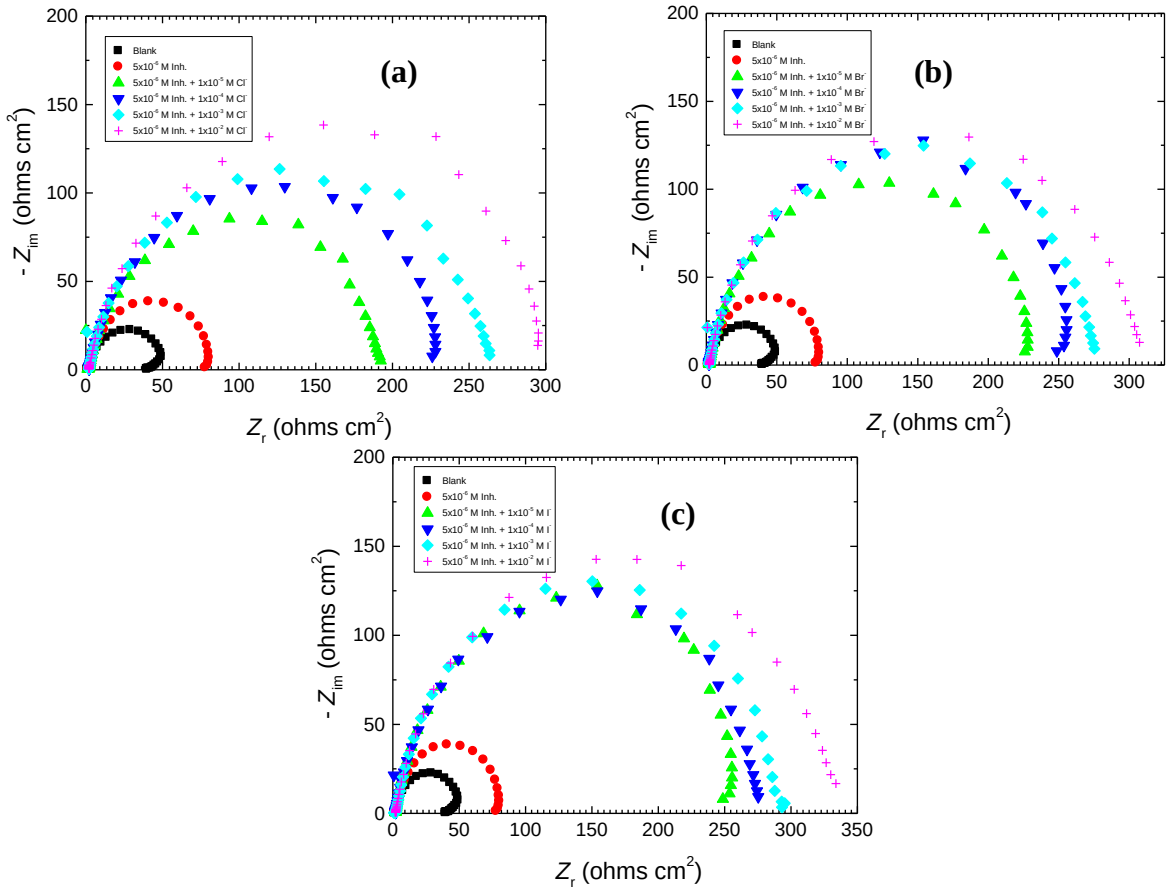

Figure 10(a-c). Effects of halides concentration on the protection efficiency (%*P*) for mild steel in 0.5 M H_2SO_4 containing $5x10^{-6}$ M AMTT inhibitor at 20 ^oC.

Table 4. Effects of halides concentration on %*PI* for mild steel in 0.5 M H_2SO_4 containing $5x10^{-6}$ M AMTT inhibitor at 20 ^oC.

	% *P*		
[X^-], M	Cl^-	Br^-	I^-
$1x10^{-5}$	74	77	79
$1x10^{-4}$	77	79	81
$1x10^{-3}$	80	81	82
$1x10^{-2}$	82	83	84

3.5. Effect of temperature and kinetic parameters

The effect of temperature on the inhibition efficiency was studied in the temperature range of 20 to 50 ^oC in 0.5 M H_2SO_4 both in the absence and presence of various concentration of AMTT

inhibitor. Values of I_{corr} and %P are listed in Table 5. The Table shows clearly that the corrosion rate increases and protection efficiency decreases with temperature. The decrease in %P with temperature suggests that physical adsorption is the predominant mechanism [33,34]. Generally the increase in temperature usually accelerates the hydrogen gas evolution in acidic medium which results in higher dissolution rate of the mild steel.

I_{corr} values were determined from the corresponding Tafel plots and subsequently the apparent activation energy were estimated from the Arrhenius plots shown in Fig. 11. The dependence of the corrosion rate on temperature is expressed as follows:

$$\ln I_{corr} = \ln A - \frac{E_a}{RT} \qquad (4)$$

where A is the Arrhenius pre-exponential constant, E_a is the activation energy, R is the universal gas constant (8.314 J mol^{-1} K^{-1}), and T is the absolute temperature (K).

Table 5. Effects of temperature on the corrosion of mild steel in 0.5 M H_2SO_4 in the absence and presence of AMTT inhibitor.

10^6 [AMTT], M	Temperature (K)											
	293			303			313			323		
	I_{corr} (μA/cm^2)	% P	θ	I_{corr} (μA/cm^2)	% P	θ	I_{corr} (μA/cm^2)	% P	θ	I_{corr} (μA/cm^2)	% P	θ
0	201	--	--	262	--	--	339	--	--	412	--	--
5	132	34	0.34	180	31	0.31	247	27	0.27	317	23	0.23
10	55	62	0.62	104	60	0.60	152	55	0.55	198	52	0.52
15	32	81	0.81	55	79	0.79	91	73	0.73	132	68	0.68
20	17	92	0.92	26	90	0.90	57	83	0.83	91	78	0.78
25	12	94	0.94	21	91	0.91	47	86	0.86	82	80	0.80

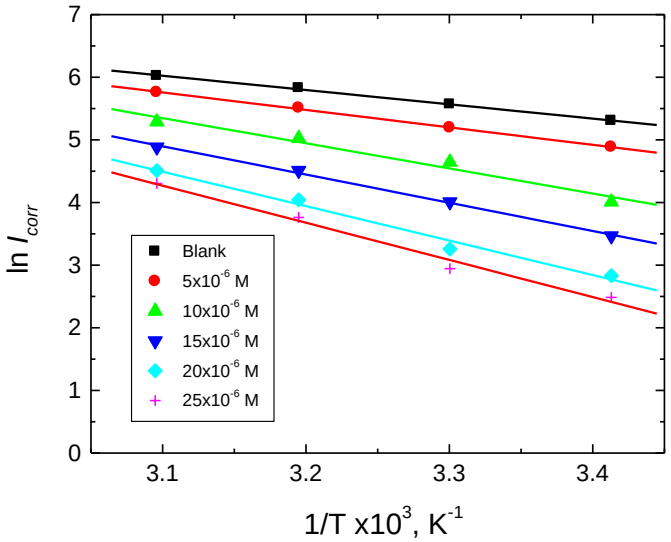

Figure 11. Arrhenius plots for the corrosion of mild steel in 0.5 M H_2SO_4 in the absence and presence of AMTT inhibitor.

Activation energy values obtained are given in Table 6. The increase in activation energy with inhibitor concentration is often interpreted by physical adsorption with the formation of an adsorptive film of an electrostatic character.

To further gain insight on the mechanism of adsorption of change of enthalpy ($\Delta H^{\#}$) and the entropy ($\Delta S^{\#}$) of activation complex in the transition state were calculated using transition state equation

$$\ln\left(\frac{I_{corr}}{T}\right)=\left(\ln\left(\frac{R}{hN}\right)+\frac{\Delta S^{\#}}{R}\right)-\frac{\Delta H^{\#}}{RT} \qquad (5)$$

where h is the Blank's constant (6.6261×10^{-34} Js), R is the universal gas constant and N is the Avogadro's number (6.0225×10^{23} mol^{-1}).

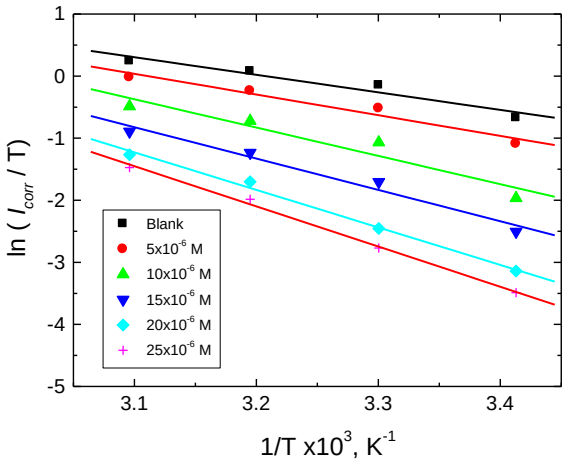

Figure 12. Transition state plots for the corrosion of mild steel in 0.5 M H_2SO_4 in the absence and presence of AMTT inhibitor.

Table 6. Activation parameters for the corrosion of mild steel in 0.5 M H_2SO_4 in the absence and presence of AMTT inhibitor.

10^6 [AMTT], M	E_a (kJ mol^{-1})	ΔH (kJ mol^{-1})	ΔS (J mol^{-1} K^{-1})	ΔG_{ads} (kJ mol^{-1})
0	18.95	23.28	-123.71	-
5	23.11	27.68	-111.41	-33.17
10	33.25	37.91	-83.14	-34.73
15	37.41	41.98	-74.24	-36.05
20	45.73	49.88	-52.04	-37.91
25	49.22	53.79	-42.82	-38.34

Figure 12 shows the plot of $\ln(I_{corr}/T)$ vs. 1/T for mild steel corrosion in 0.5 M H_2SO_4 both in the absence and presence of AMTT. Values of $\Delta H^{\#}$ and $\Delta S^{\#}$ were calculated from the slope and intercept, respectively. The positive values of $\Delta H^{\#}$ both in the absence and presence of AMTT reflect the endothermic nature of the steel dissolution process which reflects the difficulty of steel dissolution [35]. Large and negative values of $\Delta S^{\#}$ in the absence and presence of AMTT indicates that the

activation complex in the rate determining steps includes association rather than dissociation step. The negative values of ΔS_{ads} are expected as the adsorption process is accompanied by a decrease in the disorder of the system due to the adsorption of the free bulky inhibitor molecules onto the electrode surface.

3.6. Adsorption isotherm and thermodynamic parameters

The adsorption of an inhibitor is a substitutional process in which the adsorbed water molecule is being replaced by inhibitor molecules according to the following equation [36];

$$Org_{(sol)} + nH_2O(ads) \rightarrow Org_{(ads)} + nH_2O_{(sol)} \quad (6)$$

where $Org_{(sol)}$ and $Org_{(ads)}$ are the organic molecules in the aqueous solution and that adsorbed on the metal surface, respectively. $H_2O_{(ads)}$ is adsorbed water molecules and *n* is the number of water molecules replaced by one inhibitor molecule. Adsorption isotherms can provide the basic information on the interaction between the inhibitor and the mild steel surface. Four types of adsorption may take place involving organic molecules at the metal solution interface: (i) electrostatic attraction between charged molecules and the charged metal, (ii) interaction of unshared electron pairs in the molecule with the metal, (iii) interaction of *p*-electrons with the metal and (iv) a combination of the above, i.e., Inhibitor can function by physical adsorption, chemisorption or by complexation with the metal.

Attempts were made to fit experimental data to various isotherms including Langmuir, Temkin, and Flory–Huggins isotherms. It has been found that the experimental results in this study for AMTT and AMTT/halide ions systems accord with Temkin isotherm (Eq. 4) [37] and the plots are presented in Figs. 13 and 14, respectively.

$$\exp(-2a\theta) = KC \quad (7)$$

where θ is the degree of surface coverage (determined from the polarization curves shown above), *C* the inhibitor concentration, *a* the molecular interaction parameter and *K* the equilibrium constant of the adsorption process. Temkin adsorption isotherm gives an explanation about the heterogeneity formed on the metal surface.

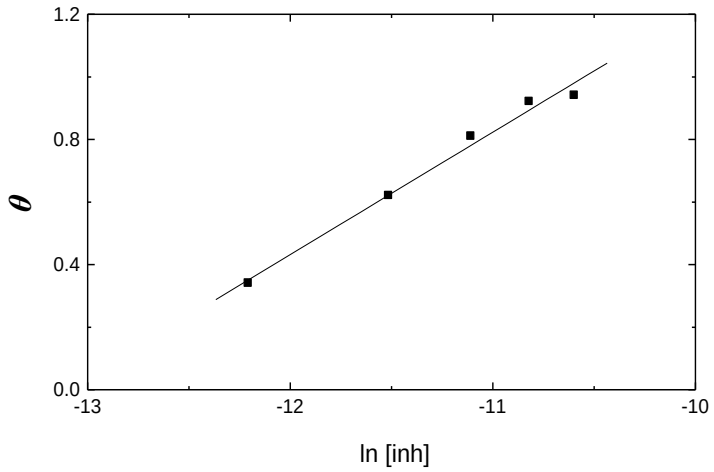

Figure 13. Temkin adsorption isotherms for AMTT inhibitor on mild steel in 0.5 M H_2SO_4 at 20 ^oC.

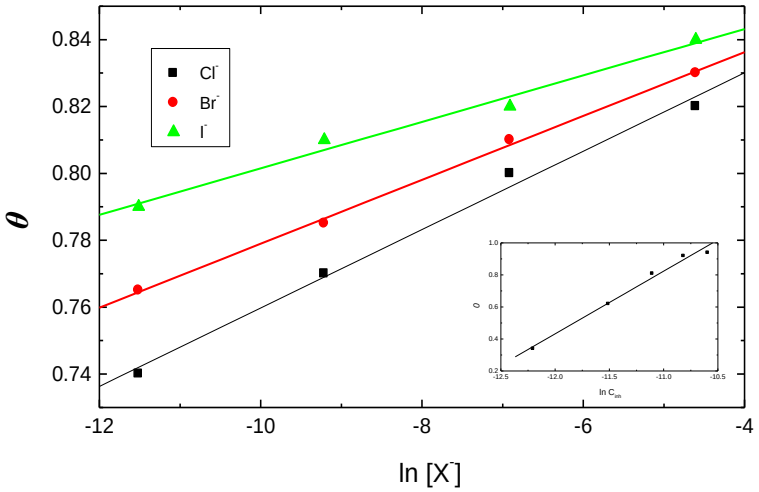

Figure 14. Temkin adsorption isotherm for AMTT inhibitor (inset) and halides on mild steel in 0.5 M H_2SO_4 at 20 ^oC.

The equilibrium constant of the adsorption process is related to the standard free energy of adsorption process by the following equation [38];

$$\Delta G_{ads} = -RT \ln(55.5K) \quad (8)$$

where 55.5 is the concentration of water expressed in mol dm^{-3}. The adsorption parameters derived from the plots are listed in Table 6. As shown in this table, *v*alues of free energy of adsorption (ΔG_{ads}) are negative and lie between-33.17 to -38.34 kJ mol^{-1}. The negative values of ΔG_{ads} reveal a spontaneous adsorption process. Generally, values of free energy of adsorption up to -20 kJ mol^{-1} are consistent with electrostatic interaction between charged molecules and a charged metal while those more negative than -40 kJ mol^{-1} involves charge sharing or transfer from the inhibitor molecules to the metal surface to form a co-ordinate type of bond. Values of ΔG_{ads} obtained in the present study are in the range -33.17 to -38.34 kJ mol^{-1}. This indicates that the adsorption of the present inhibitor involves combination of both physisorption and chemisorption [39]. In fact the adsorption process could not be classified either as purely physical or chemical. Moreover, the criteria of adsorption type obtained from the change of activation energy, shown above, cannot be taken as a decisive due to competitive adsorption with water molecules, whose removal from the surface requires also some activation energy [40,41]. Therefore, it is concluded that, the adsorption of molecules on the mild steel surface from 0.5 M H_2SO_4 solution takes place through both physical and chemical processes simultaneously.

It becomes clear that the inhibition action of AMTT at the corrosion of mild steel increases significantly in the presence of halides as revealed by the potentiodynamic polarization and electrochemical impedance spectroscopy measurements.

4. CONSLUSION

The synergistic inhibitive effect between AMTT inhibitor and halides on the corrosion of steel in 0.5 M H_2SO_4 has been studied and the following points were concluded;

1. AMTT inhibits the corrosion of mild steel in 0.5 M H_2SO_4 and it retarded both cathodic and anodic branches albeit to different extents.
2. Protection efficiency of AMTT inhibitor was increased by adding halides due to co-operative adsorption of the inhibitor and halides.
3. Experimental data were found to follow Temkin adsorption isotherm.

References

1. V.S. Sastri, Corrosion Inhibitors: Principles and Applications, Wiley, Chichester, England, 1998.
2. G. Schmitt, *Br. Corros. J.* 19 (1984) 165.
3. G. Trabanelli, *Corrosion* 47 (1991) 410.
4. Y.I. Kuznetsov, Organic Inhibitors of Corrosion of Metals, Springer, 1996.
5. R. Coughlin, Corrosion inhibitors, in: Florio, J.J., Miller, D.J., (eds.), Handbook of Coatings Additives, second ed., Marcel Dekker, New York, 2004, p. 127; W. Qafasoni, Ch. Blanc, N. Pebere, A. Srhiri, *J. Appl. Electrochem.* 30 (2000) 959.
6. C. Varalakshmi, B.V. Appa Rao, *Anticorros. Methods Mater.* 48 (2001) 171.
7. M.A. Quraish, D. Jamal, *Mater. Chem. Phys.* 68 (2001) 283.
8. S. El Hajjaji, A. Lgamri, D. Aziane, A. Guenbour, E.M. Essassi, M. Akssira, A. Ben Bachir, *Prog. Org. Coat.* 38 (2000) 207.
9. F. Bentiss, M. Lagrenee, M. Trasinel, B. Mernari, H. Elattari, *J. Appl. Electrochem.* 29, (1999) 1073.
10. M. El Achouri, S. Kertit, M. Salem, B.M. Essassi, M. Jellal, *Bull. Electrochem.* 14 (1998) 462.
11. O. Benali, L. Larabi, M. Traisnel, L. Gengembra, Y. Harek, *Appl. Surf. Sci*. 253 (2007) 6130.
12. S. Muralidharan, M.A. Quraishi, S.V.K. Iyer, *Corros. Sci.* 37 (1995) 1739.
13. M.A. Quraishi, S. Ahmad, M.Q. Ansari, *Br. Corros. J.* 32 (1997) 297.
14. A. Chetouani, B. Hammouti, A. Aouniti, N. Benchat, T. Benhadda, *Prog. Org. Coat.* 45 (2002) 207.
15. X. Li, S. Deng, H. Fu, G. Mu, *Corros. Sci.* 52 (2010) 1167.
16. A.Y. Musa, A.B. Mohamad, A.B., A.A.H. Kadhum, M.S. Takriff, L.T. Tien, *Corros. Sci.* 53 (2011) 3672.
17. A. Khamis, M.M. Saleh, M.I. Awad, *Corros. Sci.* 66 (2013) 343.
18. R. Solmaza, E. Altunbas, S. Ahin, A. Doner, G. Kardas, *Corros. Sci.* 53 (2011) 3231.
19. R. Fuchs-Godec, G. Miomir, *Corros. Sci.* 58 (2012) 192.
20. G.N. Mu, X. M. Li, F. Li, *Mater. Chem. Phys.* 86 (2004) 59.
21. R.S. Micius, M.M. Burbuliene, V. Jakubkiene, E. Udrwėnaitė, P. Vainilavičius, *J. Heterocyclic Chem.* 44 (2007) 279.
22. O.L. Riggs Jr., Corrosion Inhibitors, 2nd ed., Nathan, C.C., Houston, TX3, 1973.
23. C. Cao, *Corros. Sci.* 29 (1996) 2073.
24. Q. Qu, Z.Z. Hao, L. Li, W. Bai, Y.J. Liu, Z.T. Ding, *Corros. Sci.* 51 (2009) 569.
25. K. Aramaki, N. Hackerman, *J. Electrochem. Soc.* 116 (1969) 568.
26. L. Larabi, Y. Harek, M. Traisnel, A. Mansri, *J. Appl. Electrochem.* 34 (2004) 833.
27. S.A. Umoren, O. Ogbobe, I.O. Igwe, E.E. Ebenso, *Corros. Sci.* 50 (2008) 1998.
28. D. Asefi, M. Arami, N.M. Mahmoodi, *Corros. Sci.* 52 (2010) 794.

29. C. Jeyaprabha, S. Sathiyanarayanan, S. Muralidharan, G. Venkatachari, *J. Braz. Chem. Soc.* 17 (2006) 61.
30. M. Bouklah, N. Benchat, A. Aouniti, B. Hammouti, M. Benkaddour, M. Lagrene´e, H. Vezin, H., Bentiss, *Prop. Org. Coat.* 51 (2004) 118.
31. F. Mansfeld, M.W. Kending, S. Tsai, *Corrosion* 37 (1982) 301.
32. H. Shih, F. Mansfeld, *Corros. Sci.* 29 (1989) 1235.
33. M. Erbil, *Chim. Acta Turc.* 1 (1988) 59.
34. F. Touhami, A. Aouniti, Y. Abed, B. Hammouti, S. Kertit, A. Ramdani, K. Elkacemi, *Corros. Sci.* 42 (2000) 929.
35. M.I. Awad *J. Appl. Electrochem.* 36 (2006) 1163.
36. J.O. Bockris, D.A.J. Swinkels, *J. Electrochem. Soc*. 11 (1964) 736.
37. M. Sahin, S. Bilgic, H. Yılmaz, *Appl. Surf. Sci.* 195 (2002) 1.
38. R. Solmaza, E. Altunbas, G. Kardas, *Mater. Chem. Phys.* 125 (2011) 796.
39. S.A. Umoren, I.B. Obot, E.E. Ebenso, P.C. Okafor, O. Ogbobe, E.E. Oguzie, *Anti-Corros. Method Mater.* 53 (2006) 277.
40. L.J. Vracar, D.M. Drazic, *Corros. Sci.* 44 (2002) 1669.
41. Y. Tang, F. Zhang, S. Huc, Z. Cao, Z. Wu, W. Jing, *Corros. Sci.* 74 (2013) 271.